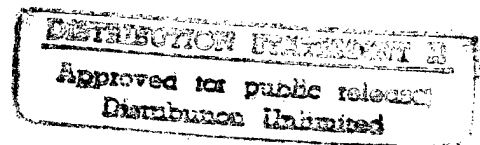


**ANNUAL REPORT**  
**TO**  
**OFFICE OF NAVAL RESEARCH**  
**Contract USN 00014-96-I-0913**  
**May 1997**

**EFFECTS OF POLLUTANTS AND MICROORGANISMS  
ON THE ABSORPTION OF ELECTROLYTIC  
HYDROGEN IN IRON**

**H. W. Pickering**  
**Department of Materials Science and Engineering**  
**The Pennsylvania State University**  
**University Park, PA 16802**

19970623 242



DTIC QUALITY

PENNSTATE



**ANNUAL REPORT**  
**TO**  
**OFFICE OF NAVAL RESEARCH**  
**Contract USN 00014-96-I-0913**  
**May 1997**

**EFFECTS OF POLLUTANTS AND MICROORGANISMS  
ON THE ABSORPTION OF ELECTROLYTIC  
HYDROGEN IN IRON**

**H. W. Pickering**  
**Department of Materials Science and Engineering**  
**The Pennsylvania State University**  
**University Park, PA 16802**

# REPORT DOCUMENTATION PAGE

Form Approved  
OMB No. 0704-0188

Public reporting burden for this collection of information is estimated to average 1 hour per response, including the time for reviewing instructions, searching existing data sources, gathering and maintaining the data needed, and completing and reviewing the collection of information. Send comments regarding this burden estimate or any other aspect of this collection of information, including suggestions for reducing this burden, to Washington Headquarters Services, Directorate for Information Operations and Reports, 1215 Jefferson Davis Highway, Suite 1204, Arlington, VA 22202-4302, and to the Office of Management and Budget, Paperwork Reduction Project (0704-0188), Washington, DC 20503.

<b>1. AGENCY USE ONLY (Leave blank)</b>	<b>2. REPORT DATE</b> May 1997	<b>3. REPORT TYPE AND DATES COVERED</b> Annual
---	-----------------------------------	---

<b>4. TITLE AND SUBTITLE</b>  Effects of Pollutants and Microorganisms on the Absorption of Electrolytic Hydrogen in Iron	<b>5. FUNDING NUMBERS</b>  USN 00014-96-I-0913
---	--

<b>6. AUTHOR(S)</b>  Howard W. Pickering	<b>7. PERFORMING ORGANIZATION NAME(S) AND ADDRESS(ES)</b> The Pennsylvania State University Department of Materials Science and Engineering 326 Steidle Building University Park, PA 16802
--	--

<b>8. PERFORMING ORGANIZATION REPORT NUMBER</b>	<b>9. SPONSORING / MONITORING AGENCY NAME(S) AND ADDRESS(ES)</b> Program Officer ATTN: A. John Sedriks, ONR 332 Office of Naval Research Ballston Centre Tower One 800 North Quincy Street Arlington, VA 22217-5660
---	---

<b>10. SPONSORING / MONITORING AGENCY REPORT NUMBER</b>	<b>11. SUPPLEMENTARY NOTES</b>
---	--------------------------------

<b>12a. DISTRIBUTION / AVAILABILITY STATEMENT</b>  Approved for public release; distribution is unlimited.	<b>12b. DISTRIBUTION CODE</b>
--	-------------------------------

**13. ABSTRACT (Maximum 200 words)**

The objective of this research is to define the conditions under which pollutants, in particular those produced by bacteria such as the sulfide end product of the SRB, affect the amount of hydrogen absorbed by iron/steel during open circuit corrosion and under cathodic polarization conditions. At the same time we will be investigating protective measures including the development of improved inhibitors that will work under occluded conditions as exist during microbiological corrosion and localized corrosion in general.

<b>14. SUBJECT TERMS</b> KEY WORDS: hydrogen absorption, steel, pollutants, sulfide, SRB, MIC, benzotriazole, crevices, cathodic protection.	<b>15. NUMBER OF PAGES</b>
--	----------------------------

<b>16. PRICE CODE</b>	<b>17. SECURITY CLASSIFICATION OF REPORT</b>	<b>18. SECURITY CLASSIFICATION OF THIS PAGE</b>	<b>19. SECURITY CLASSIFICATION OF ABSTRACT</b>	<b>20. LIMITATION OF ABSTRACT</b>
-----------------------	--	---	--	-----------------------------------

An aqueous corrosion reaction can be described by one or more cathodic and anodic partial reactions. The anodic reaction is metal dissolution which can be represented by



The cathodic reaction consumes the electrons liberated from the anodic reaction. In aqueous corrosion there are two major cathodic reactions, the hydrogen evolution reaction (HER) and the oxygen reduction reaction. The HER can be represented by the following set of equations:



and the oxygen reduction reaction by



The deterioration of the mechanical properties of the metallic structure is not only due to the dissolution of the metal according to Reaction (1) but also due to the absorption of hydrogen into the metallic lattice as a result of the HER. The absorption reaction is represented by



This absorbed hydrogen accumulates in the metallic lattice at regions of high stress triaxiality such as dislocations, inclusions and microcracks. Eventually, the metallic structure will suffer from the well known hydrogen embrittlement phenomenon and as a result, a catastrophic failure will occur.

Separation of the anodic and cathodic reactions occurs in localized corrosion, anodic reaction inside and cathodic reaction outside of the cavity, which introduces other features/complications: IR drops, solution composition changes, salt films, and solid and gaseous corrosion products. The formation of biofilms on metal surfaces can create these same conditions.

Microbiologically influenced corrosion (MIC), though not fundamentally different than other types of localized corrosion, introduces additional features as a result of the metabolism of the organisms. By attaching themselves to metal surfaces, the organisms form discrete deposits or uniform biofilms and their end products cause corrosion or accelerate existing corrosion processes.

For example, an end product of sulfate reducing bacteria (SRB) is sulfide. The biofilm provides an intimate contact between the SRB, sulfide ( $\text{H}_2\text{S}$ ,  $\text{HS}^-$  or  $\text{S}^{=}$  depending on the pH) and the steel surface. The anodic reaction then produces iron sulfide,



and the overall reaction can be represented as



in the confines of the biofilm, or the cathodic reaction can be reduction of an oxidant (e.g., oxygen via Reaction 4) operating outside of the anaerobic biofilm interface (analogous to outside of a crevice). The corrosiveness of the sulfide is related to its concentration, the pH and the nature of the iron sulfide film that forms on the steel surface (varying from rather protective to non-protective). Important characteristics of the iron sulfide film are its good electronic conductivity, low overvoltage for hydrogen evolution, noble electrode potential relative to iron and defect structure.

The objective of this research is to define the conditions under which pollutants, including those produced by bacteria such as the sulfide end product of the SRB, affect the amount of hydrogen absorbed by iron/steel during open circuit corrosion and under cathodic polarization conditions. At the same time, we will be investigating protective measures including the development of improved inhibitors that will work under occluded conditions as exist during MIC and localized corrosion in general.

## EXPERIMENTAL

The samples are high purity iron membranes of thickness 0.25 mm. They are polished to 0.1  $\mu\text{m}$  alumina, degreased in acetone and rinsed with double distilled water. Then, they are annealed in pure hydrogen at 900°C for 24 hours and cooled in the same atmosphere. The hydrogen permeation cell developed by Devanathan and Stakurski is being used to measure the hydrogen absorbed in the membrane with time. The cell is composed of two compartments,

between which the iron membrane is placed to serve as a bielectrode, see fig. 1. On one side of the membrane a solution of known pH contacts the membrane and a cathodic current is applied to reduce hydrogen on it. Part of this hydrogen will evolve as molecular hydrogen gas through Reaction 3, while the rest will go into the membrane as absorbed hydrogen. This absorbed hydrogen diffuses to the other side of the membrane where an anodic potential of 0.15 mV vs Hg/HgO is applied to oxidize all the hydrogen arriving at this surface of the membrane. This oxidation current is referred to as the hydrogen permeation current. The permeation current is measured continuously during the experiment. These resulting permeation transients are being obtained for different cathodic charging currents and different concentrations of the inhibitors added to the charging solution in the cathodic compartment of the permeation cell.

## RESULTS

Results were obtained on the project during the past year on the following topics:

1. Role of aggressive ions: sulfide and chloride.

Some preliminary results have been obtained which show that sulfide ion (as HS<sup>-</sup> and S<sup>2-</sup> in alkaline and H<sub>2</sub>S in acid solutions) promotes hydrogen absorption into iron under cathodic polarization conditions. These experiments are continuing and will include characterization of FeS films on the membrane surface. Figure 2 shows some typical results.

We have recently also found that chloride ions reduce the overpotential for the HER on an iron surface in both acid and alkaline solutions at 23°C, and in turn, reduce the hydrogen coverage and permeation of hydrogen. The effects on permeation are more pronounced in alkaline than in acid solutions. Permeation transients at constant electrode potential of the charging surface and subsequent surface analyses of the uppermost atom layers of the hydrogen charged iron surface indicate (i) either a reversible or low coverage with Cl<sup>-</sup> ions, (ii) a low hydrogen coverage which is not influenced significantly by Cl<sup>-</sup> ion concentration at low overpotentials, and (iii) a marked effect of Cl<sup>-</sup> ions on reducing the hydrogen coverage of the surface and the permeability in alkaline solutions at high cathodic polarizations. Since Cl<sup>-</sup> and S<sup>2-</sup> ions are common ingredients of MIC

involving SRB, additional hydrogen permeation experiments will be conducted and hydrogen gas formation studies will be performed under occluded cell conditions with and without sulfide films on the surface.

## 2. Effect of benzotriazole on hydrogen absorption.

Benzotriazole (BTA) has been used to inhibit the hydrogen absorption and evolution reaction by iron in acidic sulfate solution of pH 1.7. The results showed that BTA acts as an inhibitor for both reactions in broad agreement with the early literature. The mechanism by which BTA inhibits the hydrogen uptake by iron was attributed to a possible decrease in the discharge rate constant of the HER, and increase in the rate constant for the recombination reaction of the HER and/or a decrease in the absorption/desorption equilibrium constant for the absorption reaction. A brief account of this work is described in the attached paper: M. H. Abd Elhamid, B. G. Ateya and H. W. Pickering, *J. Electrochemical Soc.*, 144(4), L58, 1997.

## 3. Effect of adding iodide to BTA on the hydrogen absorption reaction.

Iodide ions are known to work synergetically with BTA to inhibit the general corrosion of copper. Furthermore, the addition of iodide to some organic compounds was found to improve the inhibitive properties of such compounds towards the hydrogen absorption reaction on iron. This is in contrast to the effect of iodide by itself on the hydrogen absorption reaction of iron for which iodide is known to enhance the hydrogen absorption reaction. Thus, it was thought that iodide ions might work synergistically with BTA to inhibit the hydrogen absorption reaction on iron. Results obtained, however, show that the addition of iodide ions to a 10 mM solution of BTA enhances, rather than inhibits, the hydrogen absorption reaction on iron. Fig. 3 shows the effect of adding iodide to the BTA solution on the hydrogen permeation transients obtained at different cathodic charging currents.

## 4. Effect of adding $\text{Cu}^{2+}$ to BTA on the hydrogen absorption and evolution reactions on iron.

Recently, there has been some work in the literature showing the inhibitive properties of a mixture of BTA and  $\text{Cu}^{2+}$  ions on the corrosion of cobalt. The mixture inhibits the corrosion of cobalt better than BTA by itself. The improved inhibiting performance was attributed to the

formation of a  $\text{Cu}^+/\text{BTA}$  complex on the cobalt surface. Tests are underway to test for the effect of adding  $\text{Cu}^{2+}$  ions to BTA on the hydrogen absorption and evolution reaction on iron. Fig. 4 shows several permeation transients obtained in the presence of 10 mM BTA and different concentrations of  $\text{Cu}^{2+}$  ions, 0.01 mM and 0.1 mM. Fig. 4 reveals that the addition of 0.01 mM  $\text{Cu}^{2+}$  to the BTA solutions decreases the permeation current. Further decrease was obtained in the presence of 0.1 mM  $\text{Cu}^{2+}$  ions. Fig. 5 shows Tafel plots obtained in the presence of BTA at different concentrations of the  $\text{Cu}^{2+}$  ions and reveals that the addition of  $\text{Cu}^{2+}$  ions to the BTA solution also increases the effectiveness of BTA towards inhibiting the HER. This can be recognized by the increase in the cathodic potential at the same cathodic current after adding the  $\text{Cu}^{2+}$  ions, to the 10 mM BTA solution. Further proof for the effect of the  $\text{Cu}^{2+}$  ions on the effectiveness of BTA towards the hydrogen absorption and evolution reactions on iron can be seen in Fig. 6. It shows the relation between the steady state permeation current and the cathodic potential at different charging solution compositions, blank, 10 mM BTA, 10 mM BTA + 0.01 mM  $\text{Cu}^{2+}$  and 10 mM BTA + 0.1 mM  $\text{Cu}^{2+}$  ions. At -0.7V (SCE) the steady state permeation current decreases by an order of magnitude from that for the blank solution after adding 0.01 mM  $\text{Cu}^{2+}$  to the BTA solution. A further decrease was achieved in the presence of 0.1 mM  $\text{Cu}^{2+}$  ions. The same effect for the copper ions on the effectiveness of BTA towards the hydrogen absorption reaction was obtained when the sample was left in contact with the charging solution at the open circuit potential, see Fig. 7.

This effect of  $\text{Cu}^{2+}$  ions could be understood in the light of the formation of a  $\text{Cu}^+/\text{BTA}$  film on the iron surface. This film will interfere with the HER by decreasing the rate of its discharge reaction, Equation (2), or by decreasing the rate of the hydrogen absorption reaction represented by Equation (5). Alternatively, the same effect could be obtained if Cu atoms are deposited on the surface of the iron membrane since Cu is a fcc metal which has a low diffusivity for hydrogen. Experiments with  $\text{Cu}^{2+}$  ions in the absence of BTA, however, reveals that the deposition of Cu on the iron surface cannot account for the decrease in the steady state permeation current achieved with  $\text{Cu}^{2+}$  ions in the presence of BTA, see Fig. 8. Accordingly, the  $\text{Cu}^{2+}$  ions work synergistically

with BTA to inhibit the hydrogen absorption reaction on iron either by the formation of a complex film on the iron surface or by the absorption of BTA on the deposited copper atoms on the iron surface which also might lead to the same complex film. Further experiments will be carried out to unravel the mechanism by which the  $\text{Cu}^{2+}$  ions increase the effectiveness of BTA towards inhibiting the HER and the hydrogen absorption reaction on iron. The ions of other metals, in particular  $\text{Zn}^{2+}$ , will be similarly evaluated.

## PUBLICATIONS ON THE PROJECT

1. A. M. Allam, B. G. Ateya and H. W. Pickering, "Effect of Chloride Ions on the Absorption and Permeation of Hydrogen in Iron," *Corrosion*, 53, 284 (1997).
2. B. G. Ateya and H. W. Pickering, "The Interaction Between the IR Potential Drop and Composition Changes During the Activation and Propagation of Crevice Corrosion", *Proc. Corrosion 96, Research Topical Symposia, Part II - Crevice Corrosion: The Science and Its Control in Engineering Practice*, NACE International, Houston, TX (1996), pp. 341-354.
3. M. H. Abd Elhamid, B. G. Ateya and H. W. Pickering, "Benzotriazole as an Inhibitor for the Hydrogen Uptake by Iron, :Extended Abstracts, Vol. 96-2, The Electrochemical Society, Pennington, NJ (Oct. 6-11, 1996, San Antonio, TX).
4. M. H. Abd Elhaamid, B. G. Ateya and H. W. Pickering, "Effect of Benzotriazole on the Hydrogen Absorption by Iron", *J. Electrochem. Soc.*, 144, L58-L61 (1997).

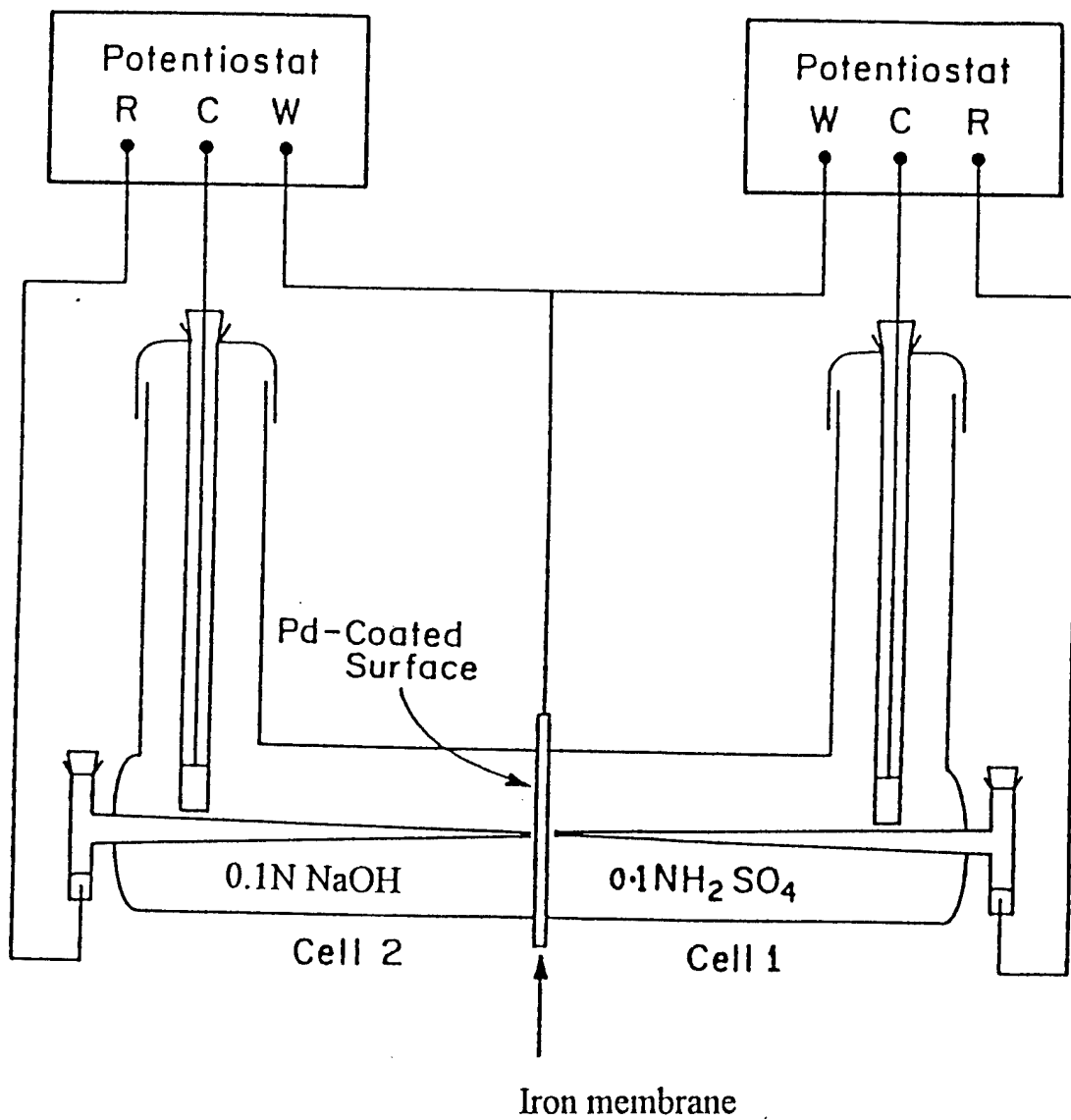


Fig.1 Schematic illustration of the electrochemical permeation cell.

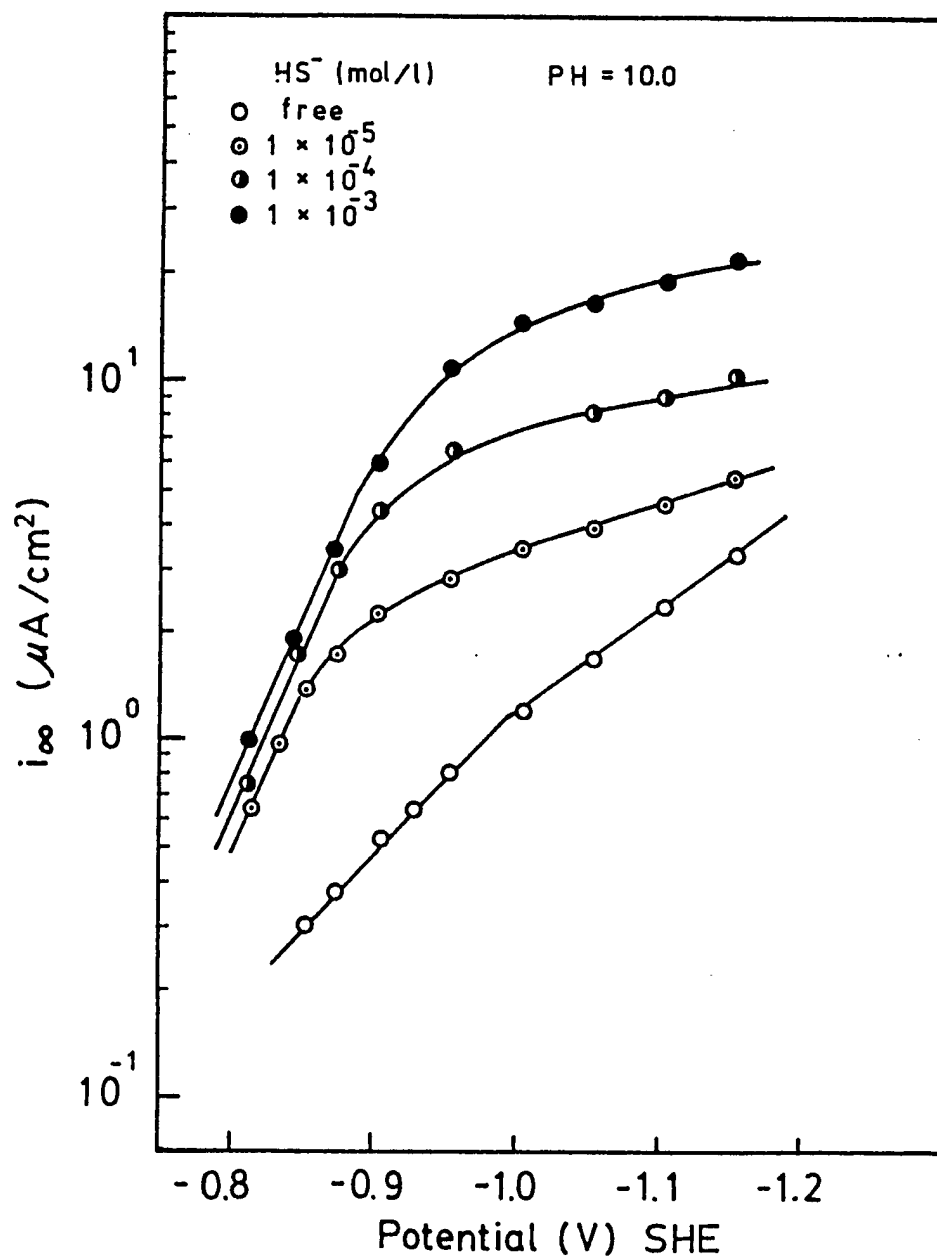


Figure 2. Effect of the  $\text{HS}^-$  ion on the steady state hydrogen permeation current,  $I_{\infty}$ , over a range of cathodic potentials in a pH 10 solution.

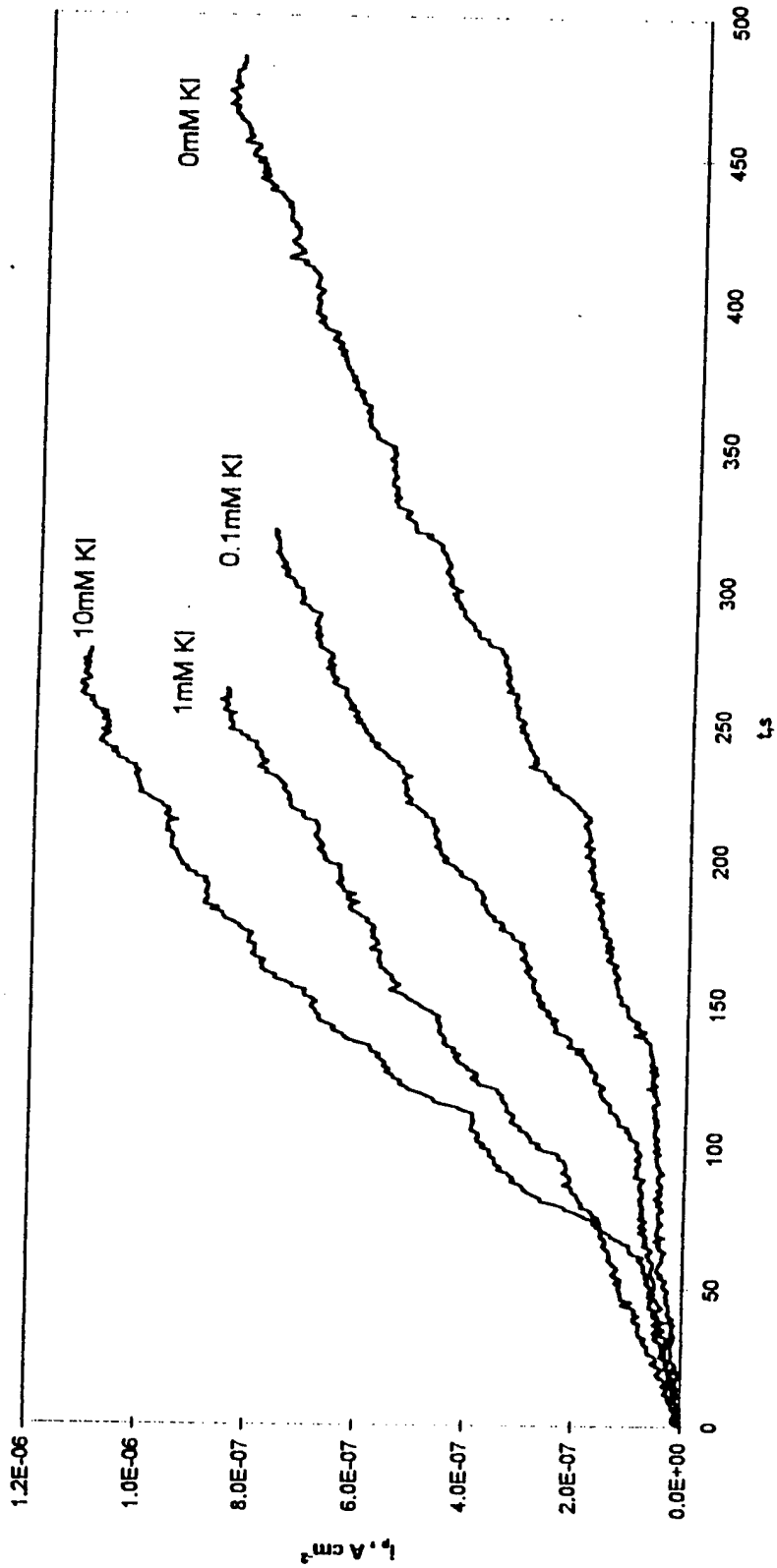


Figure 3. Effect of the addition of the iodide ion to 10 mM BTA in a 0.1 N  $\text{H}_2\text{SO}_4$  + 0.9 N  $\text{NaSO}_4$  solution on the rate of hydrogen permeation,  $i_p$ , through iron during the experiment.

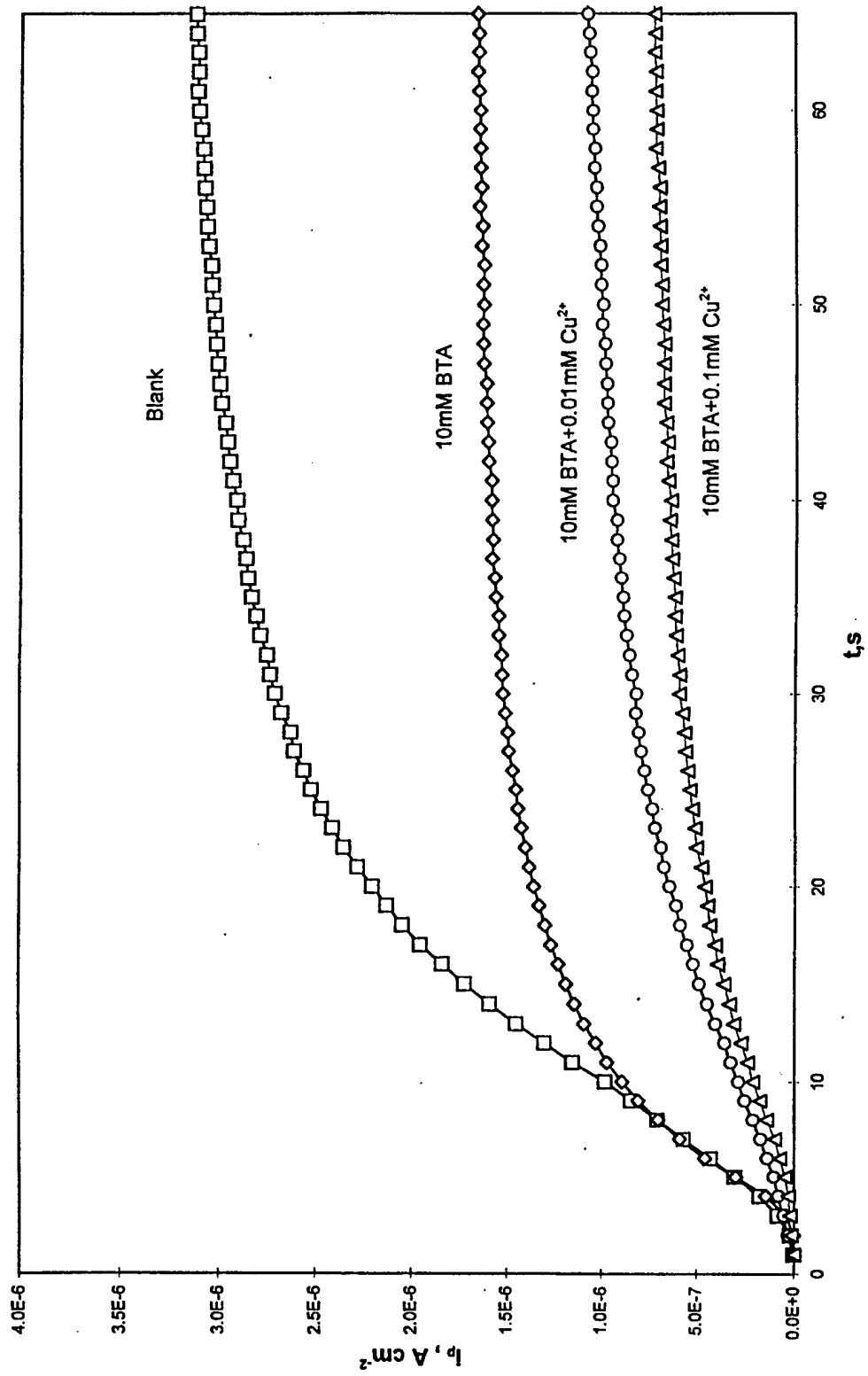


Figure 4. Hydrogen permeation transients obtained at different charging solution compositions on iron at a cathodic current density of 1.25 mA cm<sup>-2</sup>.

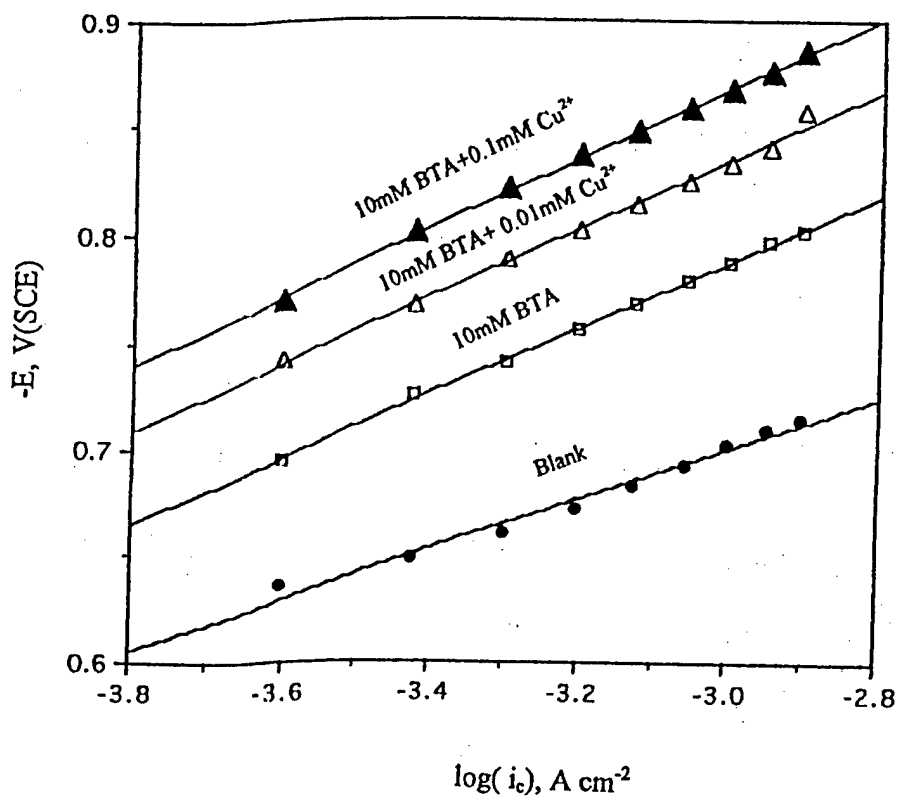


Figure 5. Tafel plots obtained at different charging solution compositions.

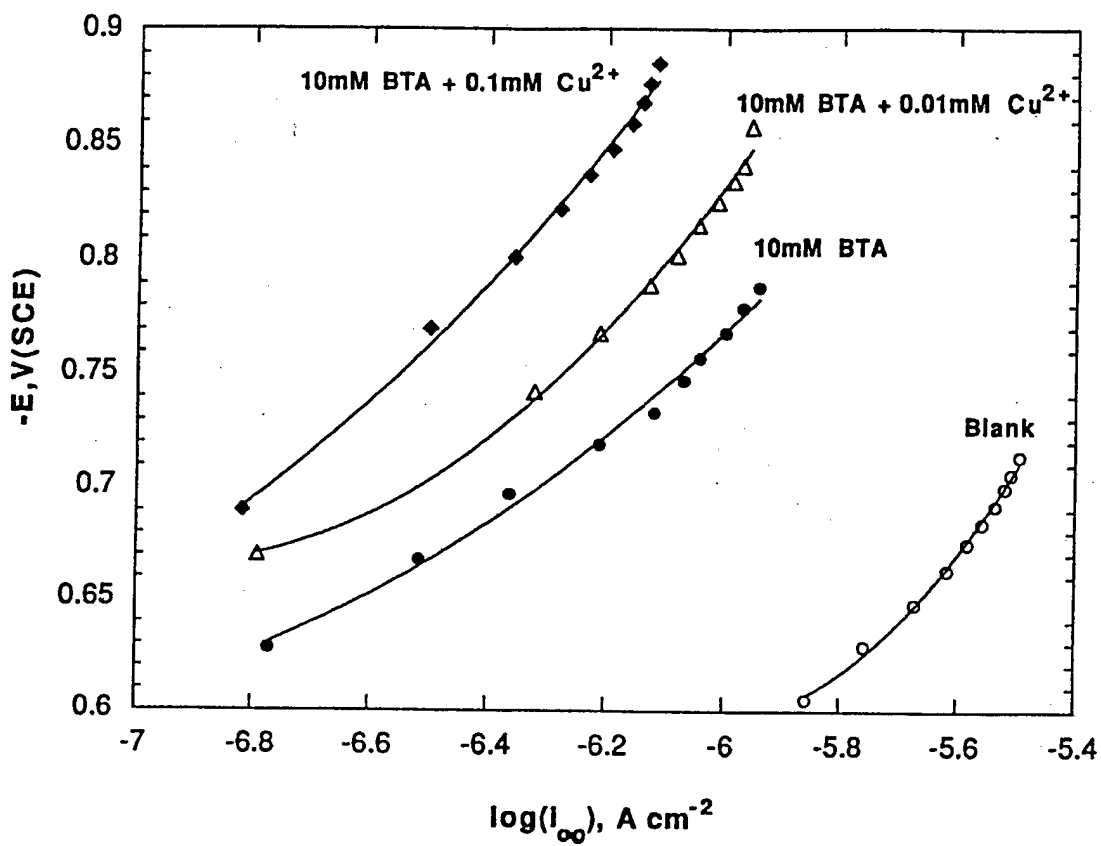


Figure 6. The relation between the cathodic potential at the charging side of an iron membrane and the steady state permeation current at different charging solution compositions.

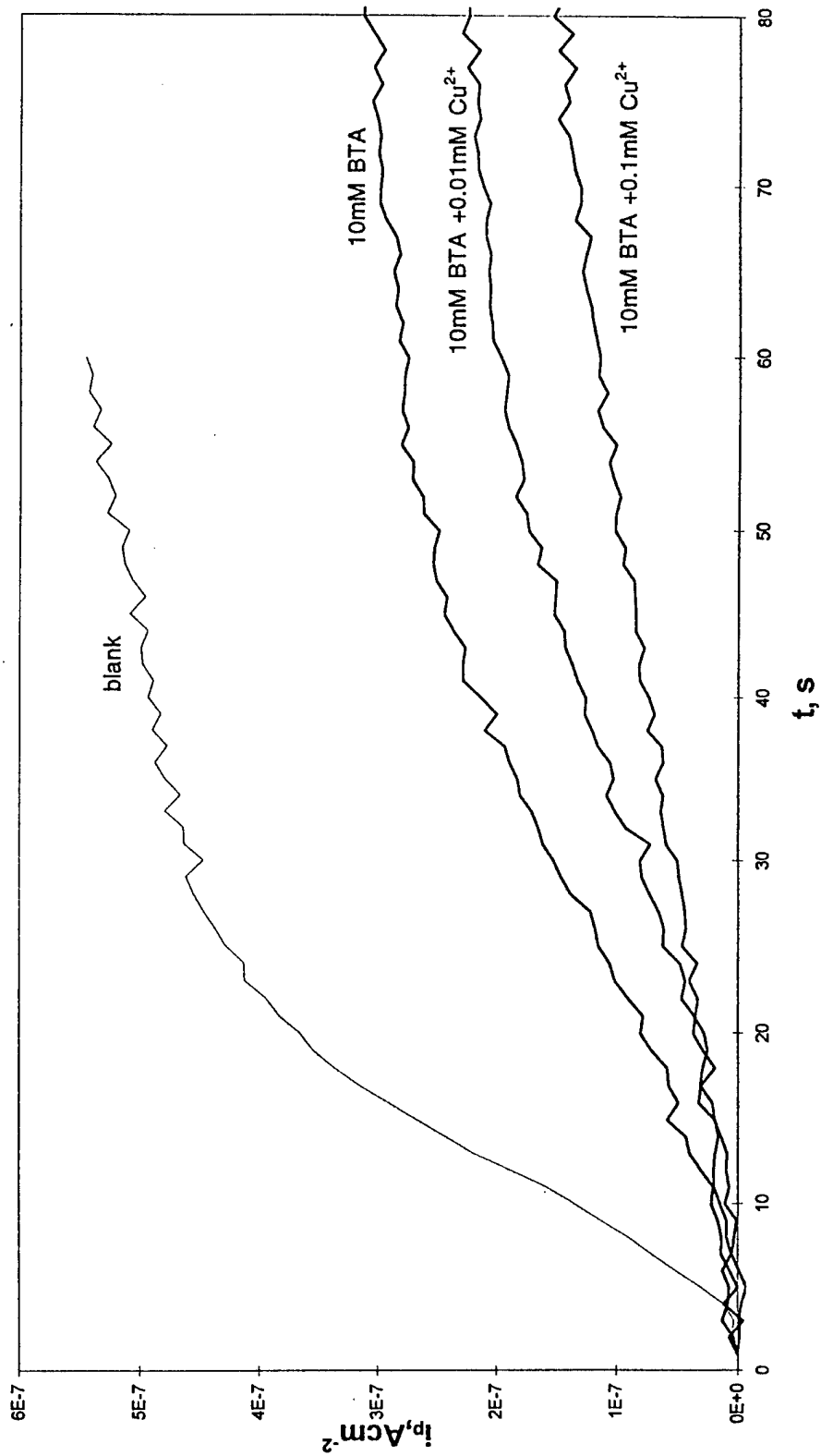


Figure 7. Permeation transients obtained on an iron membrane at different charging solution compositions with the membrane left at the open circuit potential.

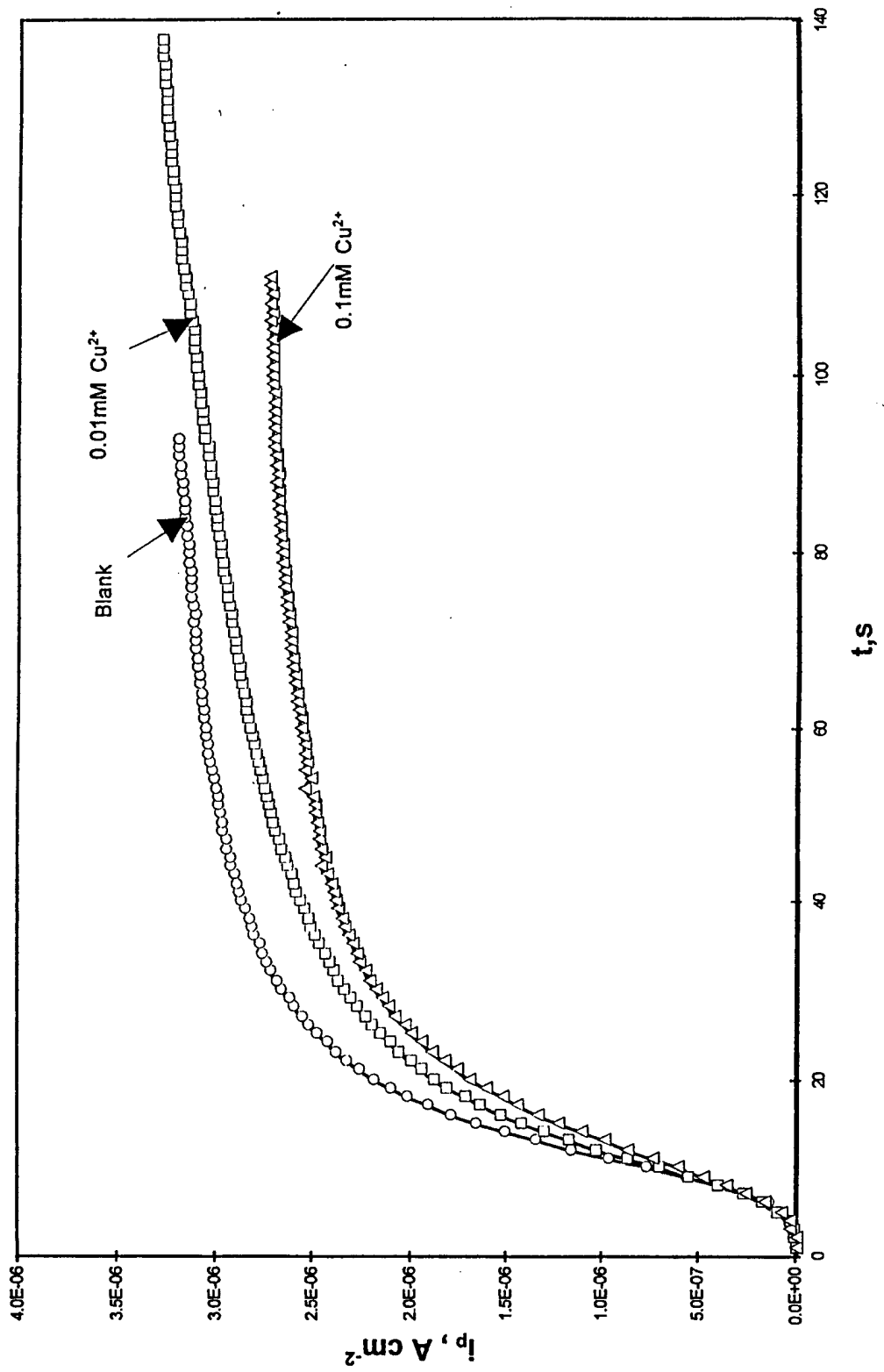


Figure 8. Permeation transients obtained on an iron membrane at different charging solution compositions on an iron membrane at a cathodic current density of  $1.25\ mA\ cm^{-2}$ .

# Effect of Benzotriazole on the Hydrogen Absorption by Iron

M. H. Abd Elhamid,<sup>\*,a</sup> B. G. Ateya<sup>\*\*,b</sup> and H. W. Pickering<sup>\*\*\*,a</sup>

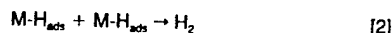
<sup>a</sup>Department of Materials Science and Engineering, Pennsylvania State University, University Park, Pennsylvania 16802, USA  
<sup>b</sup>Department of Chemistry, Faculty of Science, Cairo University, Cairo, Egypt

## ABSTRACT

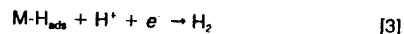
The results presented show that benzotriazole (BTA) inhibits the absorption of hydrogen into iron which is cathodically polarized in an acid (pH ≈ 1.7) sulfate solution. Analysis of the results indicates that BTA inhibits also the hydrogen evolution reaction, although it does not change its mechanism, which is shown to be proton discharge-Tafel recombination. However, BTA shifts the position of the equilibrium,  $H_{ads} \rightleftharpoons H_{abs}$ , toward the left side and hence leads to a decrease in the concentration of  $H_{abs}$  within the lattice. The extent of this decrease depends on the BTA concentration, e.g., about fivefold at 1 mM and tenfold at 10 mM BTA. This effect is opposite to that reported for inhibitors such as thiourea which inhibits the hydrogen evolution reaction and yet promotes hydrogen permeation.

## Introduction

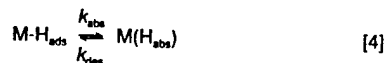
The absorption of hydrogen in metals and alloys is a precursor to hydrogen embrittlement, the deterioration of the materials mechanical properties, and failure by crack propagation.<sup>1,2</sup> The problem is hardly avoidable since hydrogen enters metals and alloys from many sources, e.g., corrosion, acid pickling, electroplating, welding, cathodic protection. In aqueous environments, the introduction of hydrogen within the metal or the alloy occurs during the hydrogen evolution reaction (HER).<sup>3,6</sup> There are two generally accepted mechanisms for this reaction<sup>3,6,7</sup>: the discharge-Tafel recombination



and the discharge-electrochemical desorption which begins with reaction 1 followed by



where  $M-H_{ads}$  refers to a nascent hydrogen atom adsorbed on the metal surface. The major part of this adsorbed hydrogen reacts to give hydrogen molecules through reactions 2 or 3. A fraction of this adsorbed hydrogen is adsorbed into the metallic lattice,  $M(H_{abs})$



This adsorbed hydrogen diffuses within the metal and eventually causes embrittlement. Many theories have been proposed to explain the phenomenon, e.g., the pressure theory, the adsorption theory, the decohesion theory, and the hydride theory.<sup>1,2</sup>

Different approaches have been proposed to mitigate the problem, either by the use of inhibitors,<sup>8-15</sup> by coating the surface,<sup>16,18</sup> or alloying with elements which have lower diffusivities for hydrogen.<sup>19,20</sup> Among the inhibitors, BTA has been tested on iron<sup>9</sup> and steel<sup>10</sup> in strongly acidic media. None of these referenced works dealt with the mechanism involved in the inhibition of the hydrogen absorption process. Further, both sets of results produced different conclusions. For instance, Dull and Nobe<sup>9</sup> found that the efficiency of BTA as an inhibitor for hydrogen absorption increases significantly with the rate of hydrogen evolution, whereas Subramanyan *et al.*<sup>10</sup> found that the efficiency to be independent of the extent of cathodic polarization and hence of the rate of hydrogen evolution. These measurements were obtained in unbuffered and strongly acidic media where BTA is known to be less efficient as a general corrosion inhibitor.<sup>21</sup>

Our objective here is to explore the effect of BTA on the kinetics of the hydrogen absorption within iron. The experimental results were obtained in a buffered acidic medium of a pH at which BTA has a high efficiency as a general corrosion inhibitor. BTA is widely used as a general corrosion inhibitor for copper and its alloys<sup>22-25</sup> and to lesser extent for iron base alloys.<sup>21,26-28</sup>

## Experimental

A hydrogen permeation cell<sup>29,30</sup> was used to measure the permeability of hydrogen through iron membranes. The cell consists of two identical parts separated by the metal membrane, Fig. 1. One side and its associated circuitry were used to generate the hydrogen charging current and to measure the potential of the charging side of the membrane while the other side was used to monitor the diffusion flux of hydrogen through the membrane by measuring the hydrogen oxidation current at the exit surface of the membrane. The charging side had a saturated calomel reference electrode whereas the exit side had a Hg/HgO reference electrode. Both sides had Pt counterelectrodes, which were separated from the solution using glass frits. The exposed surface area of the sample was 0.8 cm<sup>2</sup>.

The iron membranes (0.025 cm thick) were obtained from Goodfellow with the following composition: Mn, 0.3% Si, 0.1%; C, <0.08%; S, <0.05%; and the balance is iron. They were polished successively down to 600 emery paper, degreased ultrasonically in acetone, annealed at 900°C for 2 h in pure hydrogen, and furnace cooled in the same atmosphere.

The charging solution was 0.1 N H<sub>2</sub>SO<sub>4</sub> + 0.9 N Na<sub>2</sub>SO<sub>4</sub>, pH ≈ 1.7. The solutions were prepared from analytical grade chemicals and double-distilled water. They were pre-electrolyzed at 3 mA for 24 h in external cells. All solutions were continuously deaerated with pure hydrogen.

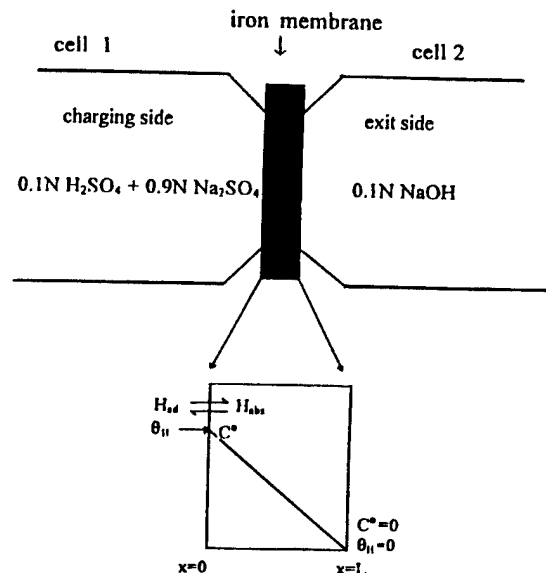


Fig. 1. Schematic illustration showing (a, top) the position of the iron membrane between the two electrolytic cells and (b, bottom) the boundary conditions imposed on the membrane by the two cells.

\* Electrochemical Society Student Member.  
 \*\* Electrochemical Society Active Member.  
 \*\*\* Electrochemical Society Fellow.

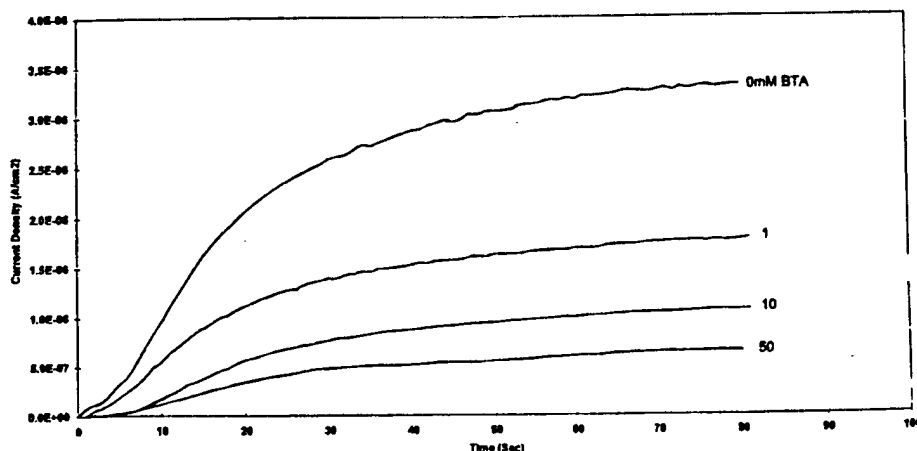


Fig. 2. Hydrogen permeation transients obtained at different BTA concentrations, at a cathodic charging current of 1.25 mA cm<sup>-2</sup>.

The exit side of the membrane was coated with a thin layer of Pd using a commercial electroless plating bath, Pallamorse. This Pd layer protects the exit side of the membrane and provides a catalytic surface for the oxidation of hydrogen. The exit side of the membrane was polarized anodically to +150 mV (Hg/HgO). The current was recorded until it decayed to a constant value, normally below 0.2 μA cm<sup>-2</sup>. The solution was introduced into the charging side of the cell under conditions of cathodic protection to protect the sample from corrosion if left at the open-circuit potential. The permeation current (anodic current at the exit surface) was recorded vs. time until a steady-state permeation current was obtained. The cathodic current at the charging surface was then increased in a stepwise fashion after reaching a steady permeation rate at each value. Other sets of experiments were conducted with charging electrolytes containing different BTA concentrations.

**Results and Discussion**

Figure 2 shows typical permeation transients obtained at a charging current density of 1.25 mA cm<sup>-2</sup> for charging electrolytes containing different BTA concentrations. The permeation current increases with time toward a limiting steady-state value, *i<sub>s</sub>*. The figure reveals that the permeability of hydrogen through iron decreases with increase of BTA concentration. Further, BTA shifts the potential at the charging side of the membrane toward more cathodic values to an extent which also depends on the BTA concentration, as shown below. Several permeation transients were obtained at different charging currents and were repeated at different BTA concentrations.

The rate of proton discharge (reaction 1) *i<sub>c</sub>* is given by

$$i_c = Fk_1 C_{H^+} (1 - \theta_H) \exp\left(-\frac{\alpha F \eta}{RT}\right) \quad [5]$$

where *k<sub>1</sub>* is the rate constant of reaction 1, *C<sub>H<sup>+</sup></sub>* is the hydrogen ion concentration, *θ<sub>H</sub>* is the degree of surface coverage of the membrane with adsorbed hydrogen, *α* is the transfer coefficient of the discharge reaction (Eq. 1), *η* is the cathodic polarization, *F* is the Faraday constant, *R* is the universal gas constant, and *T* is the absolute temperature. The rate of the (Tafel) recombination reaction (Eq. 2) is given by

$$i_r = Fk_2 \theta_H^2 \quad [6]$$

For a mechanism of the HER involving coupled proton discharge (Eq. 1)-Tafel recombination (Eq. 2), various theoretical treatments<sup>12,31-35</sup> relate the steady-state permeation (*i<sub>s</sub>*) and recombination (*i<sub>r</sub>*) currents by

$$i_s = \frac{FD}{L} \frac{k_{abs}}{k_{des}} \sqrt{\frac{i_r}{Fk_1}} \quad [7a]$$

where *D* is the diffusivity of hydrogen in the membrane and *L* is its thickness. In view of Eq. 6, the above equation also can be expressed as

$$i_s = \frac{FD}{L} \frac{k_{abs}}{k_{des}} \theta_H \quad [7b]$$

Equation 7a predicts a straight line relation between *i<sub>s</sub>* and  $\sqrt{i_r}$  where *i<sub>s</sub>* = *i<sub>c</sub>* - *i<sub>r</sub>*. Figure 3 shows several such plots at different BTA concentrations. The plots show satisfactory straight lines passing through the origin which confirm that the reaction proceeds via the Tafel recombination and that the permeation rate is controlled by hydrogen diffusion through the membrane and not by slow kinetics at the surface, i.e., Eq. 4 is in local equilibrium. Further, the slopes of the straight lines decrease, indicating lower permeation currents as the BTA concentration increases. According to the above equations, a decrease in the permeation current may be brought about by a decrease in *θ<sub>H</sub>*, and/or in the ratio *k<sub>abs</sub>*/*k<sub>des</sub>*, which is the equilibrium constant of reaction 4. This indicates that BTA either decreases the coverage of the iron surface with adsorbed hydrogen and/or diminishes the rate constant of the forward step of reaction 4. In principle, a similar effect may be observed if BTA were to increase *k<sub>des</sub>*, i.e., to favor the reverse step of reaction 4.

Figure 4 shows the *E*-log(*i*) relations of the HER obtained on iron in the presence of various concentrations of BTA. Clearly, BTA decreases the HER rate at a given potential. It also increases the Tafel slope (2.3 *RT*/*αF*) from 120 mV per current decade for the blank electrolyte to 146, 169, and 169 mV for the electrolytes containing 1, 10, and 50 mM BTA, respectively. These plots indicate that the rate-determining step of the HER is a charge-transfer reaction (i.e., proton discharge, reaction 1) with a transfer coefficient *α* equal to 0.5 for the blank electrolyte and *α* equal to 0.35 in the presence of 10 mM BTA. Reaction 2 is excluded as a possible rate-determining step, as this requires a Tafel slope of only 30 mV

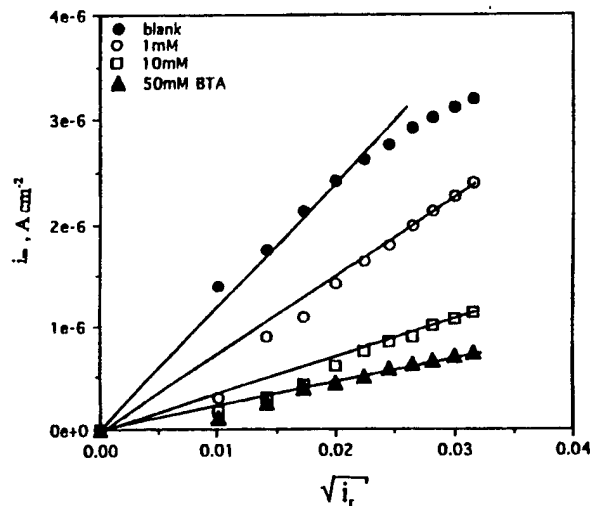


Fig. 3. Plots of the steady-state hydrogen permeation current (*i<sub>s</sub>*) vs. square root of the recombination current (*i<sub>r</sub>*) at different BTA concentrations.

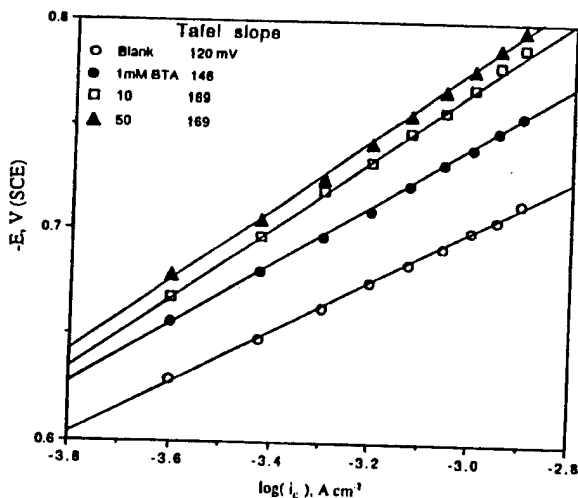


Fig. 4. Tafel plots of the hydrogen evolution reaction at different BTA concentrations.

per current decade,<sup>7</sup> which was not observed here. This analysis of Fig. 4 indicates that BTA also inhibits the HER by decreasing the rate constant of proton discharge ( $k_1$ , see Eq. 5), or the fraction of uncovered electrode area, which becomes  $(1 - \theta_H - \theta_{BTA})$ . In principle, a similar effect may be observed on a decrease in the rate of recombination (Eq. 2). If the mechanism of the HER is coupled proton discharge-Tafel recombination (Eq. 1 and 2) with both steps proceeding at comparable rates. The increase in the Tafel slope is determined solely by a decrease in  $\alpha$  (Eq. 5).

Figure 5 shows the relation between the steady-state permeation current and the cathodic potential at different BTA concentrations. It reveals that the permeation current increases at more negative (cathodic) potentials and decreases with increasing BTA concentration. This indicates that BTA inhibits the hydrogen absorption process (reaction 4) in addition to its effect of inhibiting the HER (see Fig. 4). This effect of BTA is different than that of thiourea<sup>8,35,36</sup> which inhibits the HER and promotes hydrogen absorption and that of  $H_2S^{38}$  which promotes hydrogen absorption and only mildly affects the HER. The mechanism by which such additives (poisons) promote hydrogen absorption was discussed recently<sup>37</sup> in terms of electronic interactions between the adsorbed promoters and the adsorbed hydrogen atoms on the metal surface. More work must be done to unravel the mechanism of this dual inhibitive action of BTA on the simultaneous hydrogen evolution and hydrogen absorption reactions.

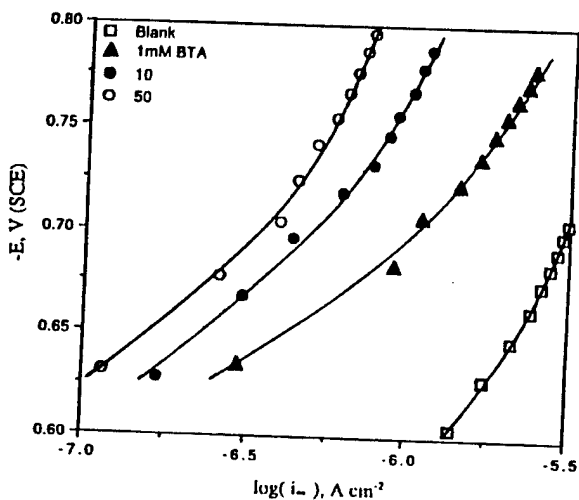


Fig. 5. Steady-state permeation current ( $I_c$ ) vs. cathodic potential ( $-E$ ) at different BTA concentrations.

Table I. Values of the steady-state permeation current,  $i_c$ , and the concentration of hydrogen in iron at the input surface,  $C^o$ , at different concentrations of the BTA at a potential of  $-0.65$  V (SCE).

[BTA], mM	$i_c$ ( $\mu A cm^{-2}$ )	$C^o$ (mol $cm^{-3}$ )
0	2.17	$4.7 \times 10^{-8}$
1	0.46	$1.0 \times 10^{-8}$
10	0.24	$5.0 \times 10^{-9}$
50	0.16	$3.5 \times 10^{-9}$

The steady-state permeation current is related to the concentration  $C^o$  by

$$i_c = FDC^o/L \quad [8]$$

where  $D$  is the diffusivity of hydrogen in the membrane of thickness  $L$ . Equation 8 reveals that the decrease in the steady-state permeation current is brought about by a decrease in  $C^o$ . This can be caused by either a decrease in  $\theta_H$  or by a shift of the equilibrium position of reaction 4 toward the left, i.e., away from  $M(H_{ads})$  toward  $M-H_{ads}$ . This conclusion is consistent with that obtained from analyzing the data in Fig. 3, in the light of Eq. 7a and b.

Equation 8 can be used to calculate the values of  $C^o$  under various conditions provided the value of  $D$  is known. We measured a diffusivity of  $1.2 \times 10^{-5} cm^2 s^{-1}$  for hydrogen in iron using the equation of breakthrough time given by Devanathan and Stachurski.<sup>30</sup> Table I lists the values of  $C^o$  so obtained at  $-650$  mV [saturated calomel electrode (SCE)] as a function of BTA concentration. As the BTA concentration increases,  $C^o$  decreases. A 10 mM BTA solution decreases  $C^o$  by about one order of magnitude.

## Conclusion

The present work shows that BTA is an efficient inhibitor for the absorption of H into iron and also for the hydrogen evolution reaction. The increase of the BTA concentration causes an increase in the cathodic polarization and in the cathodic Tafel slope on iron. It also causes a decrease in the steady-state permeation current and hence in the concentration of hydrogen in the metallic lattice. The adsorption of BTA on the iron surface leads to a marked decrease in the rate of proton discharge and a shift of the surface equilibrium  $M - H_{ads} \rightleftharpoons H_{ads}$  toward the left side which results in a decrease in the concentration of adsorbed hydrogen within the metal. This effect is opposite to that reported for some other inhibitors such as thiourea which inhibits the hydrogen evolution reaction and yet promotes hydrogen permeation. The specific effect of BTA may yet be sorted out from additional measurements and analysis.

## Acknowledgment

The authors gratefully acknowledge the encouragement and the financial assistance by the Office of Naval Research (Dr. A. J. Sedriks), Grant No. N00014-94-1-0086.

Manuscript submitted Nov. 23, 1996; revised manuscript received Jan. 31, 1997.

The Pennsylvania State University assisted in meeting the publication costs of this article.

## REFERENCES

1. H. K. Birnbaum, in *Atomistics of Fracture*, R. M. Latanision and R. M. Pickens, Editors, Plenum Press, New York (1981).
2. R. Oriani, *Corrosion*, **43**, 390 (1987).
3. M. Enyo, in *Modern Aspects of Electrochemistry*, Vol. 11, J. O'M. Bockris and B. E. Conway, Editors, p. 251, Plenum Press, New York (1975).
4. B. G. Pound, in *Modern Aspects of Electrochemistry*, Vol. 25, J. O'M. Bockris, B. E. Conway, and R. W. White, Editors, p. 63, Plenum Press, New York (1993).
5. B. K. Subramanian, in *Comprehensive Treatise of Electrochemistry*, Vol. 4, J. O'M. Bockris, B. E. Conway, E. Yeager, and R. E. White, Editors, p. 411, Plenum Press, New York (1981).
6. J. O'M. Bockris and S. U. M. Khan, *Surface Electrochemistry*, p. 833, Plenum Press, New York (1993).
7. K. J. Vetter, *Electrochemical Kinetics*, pp. 525-535, Academic Press, New York (1967).
8. D. L. Dull and K. Nobe, *Corrosion*, **35**, 535 (1979).

9. Y. Saito and K. Nobe, *ibid.*, **36**, 178 (1980).
10. N. Subramanyan, K. Balakrishnan, and B. Sathianan, in *Proceedings of the Third European Symposium on Corrosion Inhibitors*, 5, pp. 591-616 (1970).
11. S. M. Wilhelm and D. Abayarathna, *Corrosion*, **50**, 152 (1994).
12. J. O'M. Bockris, J. McBreen, and L. Nanis, *This Journal*, **112**, 1025 (1965).
13. K. Kobayashi, K. Shimizu, and M. Iida, *Corros. Sci.*, **35**, 1431 (1993).
14. R. M. Hudson and C. J. Waring, *ibid.*, **10**, 121 (1970).
15. Y. T. Al-Janabi and A. L. Lewis, *This Journal*, **142**, 2865 (1995).
16. S. S. Chatterjee, B. G. Ateya, and H. W. Pickering, *Met. Trans.*, **A9**, 389 (1978).
17. M. Zamanzadeh, A. Allam, C. Kato, B. G. Ateya, and H. W. Pickering, *This Journal*, **129**, 284 (1982).
18. D. R. Cole, G. Zheng, B. N. Popov, and R. E. White, *ibid.*, **143**, 1871 (1996).
19. J. O'M. Bockris, M. A. Genshaw, and M. Fullenwider, *Electrochim. Acta.*, **15**, 47 (1970).
20. E. Riecke, B. Johnen, and H. J. Grabke, *Werkst. Korros.*, **36**, 435 (1985).
21. R. Chin and K. Nobe, *This Journal*, **118**, 545 (1971).
22. D. Tromans and J. C. Silva, *ibid.*, **143**, 458 (1996).
23. V. Brusic, M. A. Frisch, B. N. Eldridge, F. P. Novak, F. Kaufman, B. M. Rush, and G. S. Frankel, *ibid.*, **138**, 2253 (1991).
24. C. Clerc and R. Alkire, *ibid.*, **138**, 25 (1991).
25. K. I. Kuznetsov, in *Organic Inhibitors of Corrosion of Metals*, J. G. N. Thomas, Editor, Plenum Press, New York (1996).
26. B. Sathianandhan, K. Balakrishnan, and N. Subramanyan, *Br. Corros. J.*, **5**, 271 (1970).
27. N. Eldakar and K. Nobe, *Corrosion*, **36**, 271 (1981).
28. R. Alkire and A. Cangellari, *This Journal*, **135**, 2441 (1988).
29. A. N. Frumkin and N. Aladyalova, *Acta Physicochim. (USSR)*, **19**, 1 (1944).
30. M. A. Devanathan and Z. Stachurski, *Proc. R. Soc.*, **A270**, 90 (1962).
31. M. A. Devanathan and Z. Stachurski, *This Journal*, **111**, 619 (1964).
32. C. D. Kim and B. E. Wilde, *ibid.*, **118**, 202 (1971).
33. C. Kato, H. J. Grabke, B. Egert, and G. Panzer, *Corros. Sci.*, **24**, 591 (1984).
34. R. N. Iyer, H. W. Pickering, and M. Zamanzadeh, *This Journal*, **136**, 2463 (1989).
35. B. G. Ateya and H. E. Abd Elal, in *Corrosion-Industrial Problems, Treatment and Control Techniques*, V. Ashworth, Editor, p. 201, Conf. Proc., KFAS Proc. Series, Pergamon Press, New York (1987).
36. Y. Saito and K. Nobe, *Br. Corros. J.*, **119**, 30 (1995).
37. G. Jerkiewicz, J. Borodzinski, W. Chrzanowski, and B. E. Conway, *This Journal*, **142**, 3755 (1995).

## Reports Distribution

Office of Naval Research  
Program Officer A. John Sedriks ONR 332  
Ballston Centre Tower One  
800 North Quincy Street  
Arlington, VA 22217-5660

Administrative Grants Officer  
OFFICE OF NAVAL RESEARCH REGIONAL OFFICE  
CHICAGO  
536 S. Clark Street Room 208  
Chicago, IL 60605-1588

Director, Naval Research Laboratory  
Attn: Code 2627  
4555 Overlook Drive  
Washington, DC 20375-5326

Defense Technical Information Center  
8725 John J. Kingman Road  
STE 0944  
Ft. Belvoir, VA 22060-6218